AIP Journal of Applied Physics

Improved blue-green electroluminescence of metal-oxide-semiconductor diode fabricated on multirecipe Si-implanted and annealed SiO_2 / Si substrate

Gong-Ru Lin and Chun-Jung Lin

Citation: Journal of Applied Physics **95**, 8484 (2004); doi: 10.1063/1.1739283
View online: http://dx.doi.org/10.1063/1.1739283
View Table of Contents: http://scitation.aip.org/content/aip/journal/jap/95/12?ver=pdfcov
Published by the AIP Publishing

Articles you may be interested in
Electroluminescence induced by Ge nanocrystals obtained by hot ion implantation into SiO_2
J. Appl. Phys. **106**, 106103 (2009); 10.1063/1.3262627

CO_2 laser rapid-thermal-annealing SiO_x based metal-oxide-semiconductor light emitting diode
Appl. Phys. Lett. **91**, 072103 (2007); 10.1063/1.2769962

Increase of blue electroluminescence from Ce-doped SiO_2 layers through sensitization by Gd^{3+} ions
Appl. Phys. Lett. **89**, 091908 (2006); 10.1063/1.2338892

Oxygen defect and Si nanocrystal dependent white-light and near-infrared electroluminescence of Si-implanted and plasma-enhanced chemical-vapor deposition-grown Si-rich SiO_2
J. Appl. Phys. **97**, 094306 (2005); 10.1063/1.1886274

Light emission from Al/HfO_2 / silicon diodes
J. Appl. Phys. **95**, 6486 (2004); 10.1063/1.1695604

Re-register for Table of Content Alerts

Create a profile.

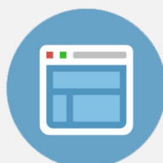

Sign up today!

[This article is copyrighted as indicated in the article. Reuse of AIP content is subject to the terms at: http://scitation.aip.org/termsconditions. Downloaded to] IP: 140.113.38.11 On: Thu, 01 May 2014 04:19:46

HTML ABSTRACT + LINKS

Improved blue-green electroluminescence of metal-oxide-semiconductor diode fabricated on multirecipe Si-implanted and annealed SiO_2/Si substrate

Gong-Ru Lin[a] and Chun-Jung Lin
Institute of Electro-Optical Engineering, National Chiao Tung University, 1001, Ta Hsueh Road, Hsinchu, Taiwan 300, Republic of China

(Received 27 October 2003; accepted 22 March 2004)

The defect-enhanced blue-green photoluminescence (PL) and electroluminescence (EL) of a metal-oxide-semiconductor (MOS) diode made on 500-nm-thick Si-ion-implanted SiO_2 ($SiO_2:Si^+$) on Si substrate are demonstrated. A multienergy/multidose implantation and 1100 °C annealing process is employed to enhance the 415–455 nm PL contributed by weak oxygen bond and neutral oxygen vacancy defects. The Ag/$SiO_2:Si^+$/n-Si/Ag MOS diode exhibits a negative-differential resistance effect with threshold field strength of 300 kV/cm. The threshold pulsed current of deep-blue EL from Ag/$SiO_2:Si^+$/n-Si/Ag diode is 280 mA (or 3 V), which turns to white-light emission at saturation current of 680 mA and further shifts to green as the biased current increases up to 3 A. The 3 dB power decay within 3 h is also observed. © *2004 American Institute of Physics.* [DOI: 10.1063/1.1739283]

The luminescent Si-rich SiO_2 (Refs. 1 and 2) materials fabricated by Si-ion implantation (referred to as $SiO_2:Si^+$) have been extensively studied, which exhibit distinguished photoluminescence (PL) at 340–550 nm (Ref. 3) and 600–900 nm.[4–7] The mechanisms of defect- and nanocrystals-Si (nc-Si)-related luminescence were subsequently investigated. The near-infrared emission are contributed by the quantum confined nc-Si embedded in $SiO_2:Si^+$.[8] In contrast, the blue-green PL peaks are mainly caused by irradiative defects, such as the weak oxygen bond[9] [O–O] (415 nm), the neutral oxygen vacancy[10] (NOV) [$O_3\equiv Si–Si\equiv O_3$] (450–470 nm), the E'_δ defect[11] [$O_3\equiv Si\uparrow Si–Si\equiv O_3$] (520 nm), and the nonbridging oxygen hole center[12] (NBOHC) [$O_3\equiv Si–O\cdot$] (620 nm). Nonetheless, the study on improving defect-related PL and electroluminescence (EL) via the modification of implantation recipe and annealing condition were less discussed. In this communication, a multiple-recipe Si-ion-implantation process is employed to obtain a uniformly Si-distributed $SiO_2:Si^+$ layer on Si substrate. Evolution of the blue-green PL spectra contributed by weak oxygen bond, NOV and E'_δ defects during different annealing periods are investigated. The current–voltage and EL characteristics of a thermally annealed Ag/$SiO_2:Si^+$/n-Si/Ag metal-oxide-semiconductor (MOS) diode are also studied.

The 500-nm-thick SiO_2 was grown on n-type (100)-oriented Si substrate by plasma enhanced chemical vapor deposition (PECVD) at a pressure of 400 mTorr with tetraethoxysilane (TEOS) fluence of 10 sccm, and O_2 fluence of 200 sccm under forward power of 150 W. The multienergy Si-implanting recipes are 5×10^{15} ions/cm^2 at 40 keV, 1×10^{16} ions/cm^2 at 80 keV, and 2×10^{16} ions/cm^2 at 150 keV (see Fig. 1). The excess Si atom density is calculated by using a Monte Carlo simulating program "TRIM." In addition, the secondary ion mass spectrometry (SIMS) of the excess Si profile in the $SiO_2:Si^+$ sample is also performed, which is in good agreement with the TRIM result. The encapsulated thermal annealing of $SiO_2:Si^+$ was performed at 1100 °C in quartz furnace with flowing nitrogen gas to activate the irradiative defects in the $SiO_2:Si^+$. The PL of $SiO_2:Si^+$ was measured using the He–Cd laser with wavelength and power density of 325 nm and 5 W/cm^2 and a fluorescence spectrophotometer (Jobin Yvon, TRIAX-320). By using a pulsed current source (ILX, LDP-3840) with period and duty cycle of 10 ms and 10%, the EL of an Ag/$SiO_2:Si^+$/n-Si/Ag MOS diode with 500 Å thick and 2 mm×2 mm square contact is measured with an optical multimeter (ILX, OMM-6810B) and an integrated sphere detector (ILX, OMH-6703B).

The PL spectra of $SiO_2:Si^+$ samples before and after annealing at 1100 °C from 1 to 4 h are shown in Fig. 2. After annealing, the PL around 410–460 nm is greatly enhanced, which is never observed from unimplanted SiO_2 and pure Si. Curve fitting of the broadband PL spectrum reveals three peak wavelengths at 415, 455, and 520 nm with associated linewidths of 35, 52, and 150 nm, respectively. The 415-nm-PL emission originates from the oxygen interstitials with weak oxygen bond.[9] The 455 nm luminescence has previously been attributed to the NOV defects. providing by the reaction of $O_3\equiv Si–O–Si\equiv O_3\rightarrow O_3\equiv Si–Si\equiv O_3 + O_{interstitial}$. The Si implantation not only induces strong displacement of the oxygen bonds but also generates enormous silicon/oxygen interstitials from the damaged lattice. Weak oxygen bond defects transfer from the oxygen interstitials after longer annealing, which is expressed by the reaction of $O_{interstitial}+O_{interstitial}\rightarrow$O–O. The E'_δ center contributes to the emission at 520 nm, which is basically a SiO_4 vacancy substituted by a single four-valent Si atom.[11] In addition, a red-shift of nc-Si dependent PL from 826 to 856.5 nm with its

[a]Electronic mail: grlin@faculty.nctu.edu.tw

[This article is copyrighted as indicated in the article. Reuse of AIP content is subject to the terms at: http://scitation.aip.org/termsconditions. Downloaded to] IP: 140.113.38.11 On: Thu, 01 May 2014 04:19:46

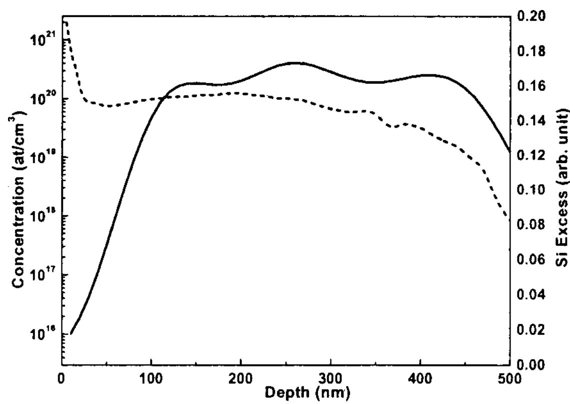

FIG. 1. Secondary ion mass spectrometry result and the TRIM-calculated excess Si-atom density in multienergy Si-ion-implanted $SiO_2:Si^+$ sample as a function of implanting depth.

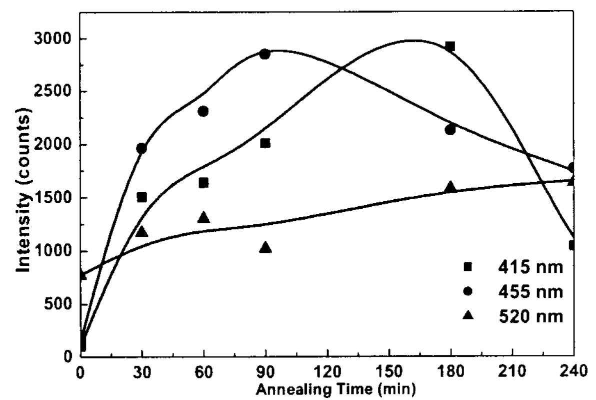

FIG. 3. Annealing-time dependent PL intensities at different wavelengths of 415, 455, and 520 nm.

maximum intensity after 3 h annealing is also observed, however, which are much weaker than those from the irradiative defects. It reveals that the present implanting dosage is insufficient to help precipitate high-density nc-Si, giving rise to a lower intensity than that attributed by the irradiative defects.

The variation in PL intensity is plotted as a function of annealing time in Fig. 3. As annealing time lengthens to 1 h, the activation of NOV defects becomes more pronounced than that of the weak oxygen bond defects. The complete activation of these irradiative defects happened after annealing for 1.5–3 h. The weak oxygen bond defect is initiated after annealing for 0.75 h, while the density of NOV defects linearly increases. After annealing for more than 1.5 h, the PL intensity of NOV defects reaches its maximum. Additional energies are required for the formation of weak oxygen bond defects from the oxygen interstitials. Although the complete activation of the NOV defect occurs earlier than that of the weak oxygen bond defect, the maximum PL intensities of both irradiative defects are within the same order, which corroborates well with the formation mechanism of oxygen vacancies and interstitials in $SiO_2:Si^+$. The damaged SiO_2 matrix is gradually regrown as the annealing time lengthens and such a crystallite recovery causes the reversed reactions.

The continuous-wave (cw) and pulsed current–voltage ($I-V$) measurement of the $Ag/SiO_2:Si^+/n$-Si/Ag MOS diode is shown in the inset of Fig. 4. The turn-on voltage and the breakdown field of the MOS diode are 2.8 V and 600 kV/cm, respectively. The cw $I-V$ measurement of the MOS diode further reveals a negative-differential-resistance effect based on carrier tunneling behavior, which has a comparable threshold field strength (300 kV/cm) to the GaN semiconductors (80–150 kV/cm).[13–15] The resistances of the $SiO_2:Si^+$ MOS diode are 7.86 and 0.6142 Ω before and after turn-on. In comparison, Yuan and co-workers[16] have observed the visible EL from Ag/native SiO_2/n-type Si substrate/Al (referred to as $Ag/SiO_2/n$-Si/Al), in which the EL occurs only under reverse bias conditions when the metal electrode is negatively biased. Bae *et al.*[1] also reported that the strong EL can only be observed in an $Au/SiO_x/p$-Si structure under reverse-biasing condition. The turn-on voltage of the diode made on $Ag/SiO_2/n$-Si/Al MOS diode is up to 50 V. Significantly, the turn-on voltage of the $Ag/SiO_2:Si^+/n$-Si/Ag diode is only 1/20 smaller than that of an $Ag/SiO_2/n$-Si/Al diode.[16] The EL emits photons via impact ionization and subsequent electron-hole recombination processes under a high electric field. The EL power of the $SiO_2:Si^+$ MOS diode driven by pulsed current from 0 to 3000 mA is also shown in Fig. 4. The threshold current and

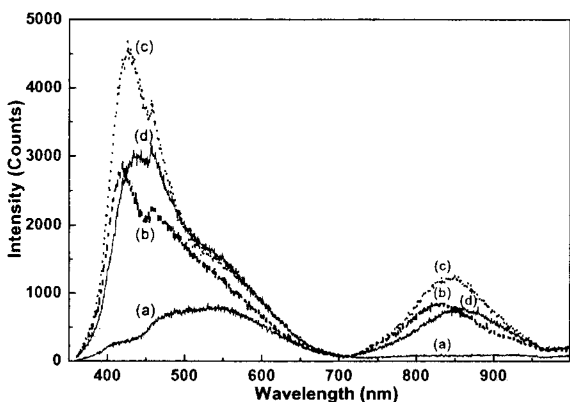

FIG. 2. PL spectra of the $SiO_2:Si^+/Si$ samples at (a) as-implanted condition, or annealed at 1100 °C for (b) 1 h (c) 3 h, and (d) 4 h.

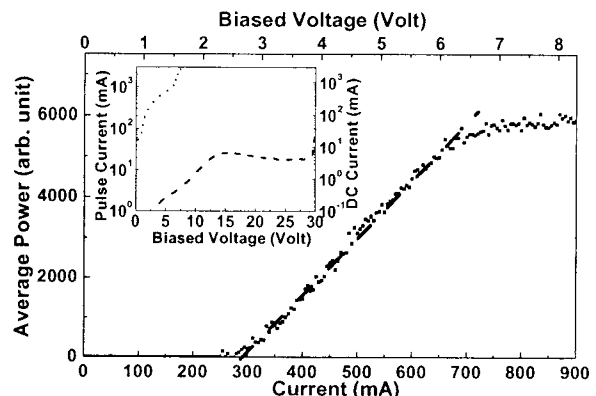

FIG. 4. Average EL power as a function of pulsed current and voltage. The inset figure shows cw (dashed line) and pulsed (dotted line) current–voltage responses of $Ag/SiO_2:Si^+/n$-Si/Ag MOS diode with $SiO_2:Si^+$ annealing at 1100 °C for 3 h.

[This article is copyrighted as indicated in the article. Reuse of AIP content is subject to the terms at: http://scitation.aip.org/termsconditions. Downloaded to] IP: 140.113.38.11 On: Thu, 01 May 2014 04:19:46

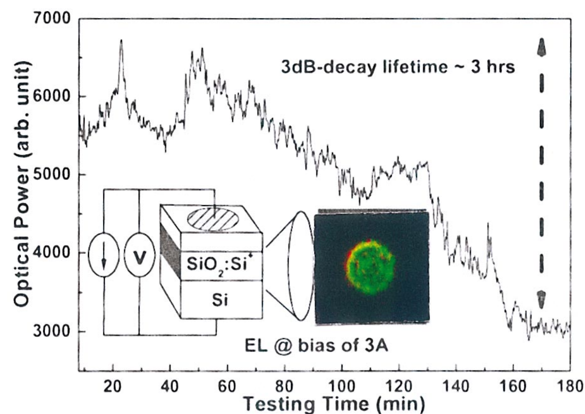

FIG. 5. (Color) Lifetime testing of $Ag/SiO_2:Si^+/n$-Si/Ag MOS diode under pulsed-current EL operation. The inset figure plots the operating condition of the MOS diode and its far-field EL pattern at bias of 3 A.

voltage of the MOS diode are 280 mA and 3 V, respectively. The average EL power is increasing to 60 nW at pumping current of 965 mA. By measuring a single luminescent point of the $Ag/SiO_2:Si^+/n$-Si/Ag diode with a lensed fiber, the power–current ($P-I$) slope is determined as 0.15 μW/A.

The EL spectrum of the $Ag/SiO_2:Si^+$/Si/Ag MOS diode is completely different from that of an $Ag/SiO_2/n$-Si/Al diode with red luminescence at 620–640 nm.[15] The far-field EL pattern of the $SiO_2:Si^+$ MOS biased at a pulsed current of 3 A is pictured and shown in the inset of Fig. 5. It is also observed that the EL patterns reveal different colors at different biased conditions. The deep-blue emission is dominated when the diode is operated at nearly threshold, which is the white-light luminescence at close to saturation condition. However, the dominated EL wavelength further lengthens to green region as the biased current increases to 2 A or larger. The enhanced EL of the $Ag/SiO_2:Si^+/n$-Si/Al sample results from the defect-to-band transition in $SiO_2:Si^+$. Both the excited states of the weak oxygen bond defects are inversely populated via the tunneling of electrons from the top metal contact and holes from Si substrate at sufficient (nearly or above threshold) bias. The tunneling electrons and holes consequently recombine and emit the luminescence. The green EL is enhanced only when the biased current (as well as the electric field) becomes extremely high, which seriously bends the inversion layer and greatly accumulates the holes beneath the $SiO_2:Si^+/n$-Si interface. This helps the tunneling of holes into NOV and E'_δ defects with higher energy levels, which correlates well with the longer EL wavelengths (455–520 nm) at higher biased conditions.

These results illustrate that the EL mechanism of the Si-rich $SiO_2:Si^+$ layer can only be initiated at reverse bias.[16] The reverse bias condition facilitates the impact ionization of ground states from the injection of the minority holes, which are accumulated in the inversion layer formed beneath the $SiO_2:Si^+/n$-Si interface. Higher electric field further provides sufficient energies for the electrons and holes to tunnel from the metal and n-Si substrate to the intermediate states in $SiO_2:Si^+$, which eventually leads to the transition from the intermediate to the ground state and attributes the blue-yellow luminescence by the E'_δ and NBOHC defects around 520–620 nm, however, such a high-field impact ionization process inevitably leads to a substrate overheating effect since the cooling of the MOS diode is not efficient. Figure 5 performs the lifetime testing of such an EL emitting diode under pulsed current of 3000 mA. The EL power of the diode with room-temperature TEC cooling has attenuated up to 58% within 3 h, which corresponds to a decaying rate of 1 dB/h.

In conclusion, by using multirecipe implantation, the defect-enhanced blue-green PL and EL of a MOS diode made on the thermally annealed Si-ion-implanted SiO_2 ($SiO_2:Si^+$) film on Si substrate with nearly flattened excess Si distribution profile are demonstrated. After long-term annealing, three strong and stable PL peaks at 415, 455, and 520 nm are observed. The optimized annealing time of 3 h for complete activation of the irradiative defects including the weak oxygen bond, the NOV, and the E'_δ centers are reported. The turn-on voltage and the breakdown field of the $SiO_2:Si^+$-based MOS diode are 2.8 V and 600 kV/cm, respectively. The EL power of the $Ag/SiO_2:Si^+/n$-Si/Ag MOS diode is linearly increased with the biased current above threshold (280 mA) and is saturated at about 680 mA. The far-field EL emission pattern of the MOS diode changes its color from deep-blue to white, and consequently to fully green at high biases. The EL lifetime testing of the MOS diode gives decaying time and rate of 3 h and 1 dB/h, respectively.

This work was supported by Dr. Jia-Min Shieh with the National Nano Device Laboratory and by the National Science Council (NSC) of the Republic of China under Grant No. NSC92-2215-E-009-028.

[1] H. S. Bae, T. G. Kim, C. N. Whang, S. Im, J. S. Yun, and J. H. Song, J. Appl. Phys. **91**, 4078 (2002).
[2] D. Pacifici, E. C. Moreira, G. Franzo, V. Martorino, and F. Priolo, Phys. Rev. B **65**, 144109 (2002).
[3] L. S. Liao, X. M. Bao, X. Q. Zheng, N. S. Li, and N. B. Min, Appl. Phys. Lett. **68**, 850 (1996).
[4] H. Z. Song and X. M. Bao, Phys. Rev. B **55**, 6988 (1997).
[5] T. S. Iwayama, K. Fujita, S. Nakao, K. Saitoh, T. Fujita, and N. Itoh, J. Appl. Phys. **75**, 7779 (1994).
[6] T. S. Iwayama, S. Nakao, and K. Saitoh, Appl. Phys. Lett. **65**, 1814 (1994).
[7] X. Zhao, O. Schoenfeld, J. Kusano, Y. Aoyagi, and T. Sugano, Jpn. J. Appl. Phys., Part 2 **33**, L648 (1994).
[8] W. Hayes, M. J. Kane, O. Salminen, R. L. Wood, and S. P. Doherty, J. Phys. C **17**, 2943 (1984).
[9] J. C. Cheang-Wong, A. Oliver, J. Roiz, J. M. Hernanaez, L. Rodriguez-Fernandez, J. G. Morales, and A. Crespo-Sosa, Nucl. Instrum. Methods Phys. Res. B **175–177**, 490 (2001).
[10] H. Z. Song, X. M. Bao, N. S. Li, and J. Y. Zhang, J. Appl. Phys. **82**, 4028 (1997).
[11] H. Nishikawa, E. Watanabe, D. Ito, Y. Sakurai, K. Nagasawa, and Y. Ohki, J. Appl. Phys. **80**, 3513 (1996).
[12] G. G. Qin, A. P. Li, B. R. Zhang, and B. C. Li, J. Appl. Phys. **78**, 2006 (1995).
[13] S. Tong, X. N. Liu, T. Gao, and X. M. Bao, Appl. Phys. Lett. **71**, 698 (1997).
[14] E. Alekseer and D. Pavlidis, Solid-State Electron. **44**, 941 (2000).
[15] G.-R. Lin, Jpn. J. Appl. Phys., Part 2 **41**, L1379 (2002).
[16] J. Yuan and D. Haneman, J. Appl. Phys. **86**, 2358 (1999).

[This article is copyrighted as indicated in the article. Reuse of AIP content is subject to the terms at: http://scitation.aip.org/termsconditions. Downloaded to] IP: 140.113.38.11 On: Thu, 01 May 2014 04:19:46